Dynamic Molecular Surface Areas

Kenny B. Lipkowitz,* Brian Baker, and Raima Larter

Contribution from the Department of Chemistry, Indiana University-Purdue University at Indianapolis, Indianapolis, Indiana 46205-2820. *Received March 2, 1989*

Abstract: The solvent-accessible surface areas for weakly bound diastereomeric complexes are computed. It is found that traditional static surfaces are inappropriate for determining differences between diastereomeric complexes. A more suitable value is an averaged dynamic solvent-accessible surface area that accounts, in a statistical way, for all low-energy structures of the complex. The dynamic surface area of the more stable diastereomeric complex is always equal to or greater than that of the less stable complex.

It has been pointed out that a molecular surface, albeit not an observable, is not unreal.[1] Although a variety of different types of molecular surfaces have been defined,[2] especially for quantitative structure–activity relationships (QSAR),[3] one of the most extensively employed is the solvent-accessible surface area, which is used for, among other reasons, determining protein folding and for predicting solubilities of drug molecules.[4] The accessible surface area, first defined by Lee and Richards,[5] is the locus of the center of a solvent "sphere" which is rolled over the van der Waals surface of the solute.[6] Computation of a molecular surface area until recently has not been amenable to analytical solution;[7] it is usually solved numerically by a variety of methods, and all studies to date share a common theme. They all invoke a single structure, even for conformationally flexible molecules.[8]

The molecular structure typically used for the calculation of the surface area is obtained from a crystallographic study or, more commonly, is the global minimum on a potential energy surface that has been suitably searched. Thus the surface area used in most analyses is a static quantity. This was pointed out by Lee and Richards in their seminal paper on the topic.[5] Because many molecules of interest are flexible and since it is evident that different molecular conformations can result in different solvent-accessible surface areas, we ask here what the differences are between a static solvent-accessible surface area (S_S) and a solvent-accessible surface area that accounts, in a statistically averaged way, for multiple conformations of a molecule. This latter quantity we define as an averaged dynamic surface area, $\bar{S}_D$.

Although dynamic literally means time dependent we are less interested in the temporal or time-dependent evolution of the molecular surface than in the spatial characteristics of the surface over a long time period. The experimental data with which we compare the results of our simulations are measurements made over a long interval of time (minutes). In this paper we sample all the configurations the system will visit over an infinite time period and use these configurations, in a statistically averaged way, to calculate an averaged property. We refer to $\bar{S}_D$ as an averaged dynamic surface area because it accounts for the likelihood of finding the system in a given state over a long time period.

Methods

1. Systems Studied. The molecules we select for our study are truly flexible; they are weakly bound diastereomeric complexes. Diastereomeric complexes form when an optically pure receptor is allowed to interact with one of two enantiomeric substrates. This scenario exists when optical analytes bind to chiral stationary phases used in chiral chromatography.[9] Our interests in chiral chromatography lead us to develop a computational protocol for determining which of two optical analytes is longer retained on a chiral column[10] and to explain, with atomistic modeling techniques, how enantiodifferentiation takes place.[11] The complexes we study in this paper arise from coordination of analytes A1–A6 with chiral stationary phase analogues CSP1 or CSP2 depicted in Figure 1.[12] CSP1 and CSP2 are truncated models of the commercially available (*R*)-phenylglycine and (*S*)-naphthylvaline Pirkle phases, respectively.[13]

2. Computational Approach. As mirror image isomers encounter a chiral stationary phase during their transit through the column, they form short-lived diastereomeric complexes. The free energy of each diastereomeric complex is approximated as $\bar{E}$, the column-averaged interaction energy, and is computed as

$$\bar{E} = \sum_{h=1}^{l}\sum_{i=1}^{m}\left(\frac{e^{-E_{CSP,h}/kT}}{\sum_{h'=1}^{l} e^{-E_{CSP,h}/kT}}\right)\left(\frac{e^{-E_{A,i}/kT}}{\sum_{i'=1}^{m} e^{-E_{A,i}/kT}}\right)\sum_{j=1}^{n} g_{hij}\left(\frac{e^{-\epsilon_{hij}/kT}}{\sum_{j'=1}^{n} e^{-\epsilon_{hij'}/kT}}\right) \quad (1)$$

The definitions and theoretical underpinning for this have been published.[10] Here we point out that the free energy depends on the shape of the chiral stationary phase (CSP), the shape of the analyte (A), and the orientation of the two relative to one another. Equation 1 reflects our concern that many CSPs are flexible

(1) Schaäfer, L. *J. Mol. Struct.* **1983**, *100*, 51.
(2) References to the various representations used for molecular shape can be found in: Arteca, G. A.; Mezey, P. G. *J. Comput. Chem.* **1988**, *9*(5), 554–563.
(3) An introductory review about molecular surface areas and their uses in structure–activity relationships exists: Pearlman, R. S. In *Physical Chemical Properties of Drugs*; Medicinal Research Series Vol. 10; Yalkowsky, S. H., Sinkula, A. A., Valvani, S. C., Eds.; Marcel Dekker: New York, 1980; Chapter 10.
(4) Camilleri, P.; Watts, Simon, A.; Boraston, J. A. *J. Chem. Soc., Perkin Trans. 2* **1988**, 1699–1707 and references therein.
(5) Lee, B.; Richards, F. M. *J. Mol. Biol.* **1971**, *55*, 379–400.
(6) Richards, F. M. *Methods Enzymol.* **1985**, *115*, 440–464.
(7) (a) Connolly, M. L., *J. Appl. Crystallogr.* **1983**, *6*, 548–558. (b) Richmond, T. J. *J. Mol. Biol.* **1984**, *178*, 63–89.
(8) To our knowledge the only work reported where multiple conformations were used to determine surface areas was that of Hermann. Hermann, R. B. *J. Phys. Chem.* **1972**, *76*(19), 2754–59.
(9) (a) Souter, R. W. *Chromatographic Separation of Stereoisomers*; CRC Press: Boca Raton, FL, 1985. (b) *Chromatographic Chiral Separations*; Chromatographic Science Series Vol. 40; Zief, M., Crane, L., Eds.; Marcel Dekker: New York, 1987. (c) Konig, W. A. *The Practice of Enantiomer Separation by Capillary Gas Chromatography*; Huethig Publishing: Heidelberg, 1987. (d) Allenmark, S. G. *Chromatographic Enantioseparation. Methods and Application*; Ellis Horwood Series in Advanced Analytical Chemistry; Chalmers, R. A., Masson, M., Eds.; Ellis Horwood Ltd.: Chichester, 1988.
(10) Lipkowitz, K. B.; Demeter, D. A.; Zegarra, R.; Larter, R.; Darden, T. *J. Am. Chem. Soc.* **1988**, *110*(11), 3446–52.
(11) Lipkowitz, K. B.; Baker, B.; Zegarra, R. *J. Comput.* **1989**, *10*(5), 718–32.
(12) The six simulations described here are reported in a full paper: Lipkowitz, K. B.; Baker, B. *Anal. Chem.*, submitted. The computed free energy differences between diastereomeric complexes have been compared with experimental separability factors, α, by $\Delta\bar{E} = -RT \ln \alpha$. A linear correlation is found between experiment and theory with a correlation coefficient for the six simulations of 0.77.
(13) (a) Pirkle, W. H.; Pochapsky, T. C.; Mahler, G. S.; Field, R. E. *J. Chromatogr.* **1985**, *348*, 89. (b) Pirkle, W. H.; Pochapsky, T. C.; Mahler, G. S.; Corey, D. E.; Reno, D. S.; Alessi, D. M. *J. Org. Chem.* **1986**, *51*, 4991.

0002-7863/89/1511-7750$01.50/0

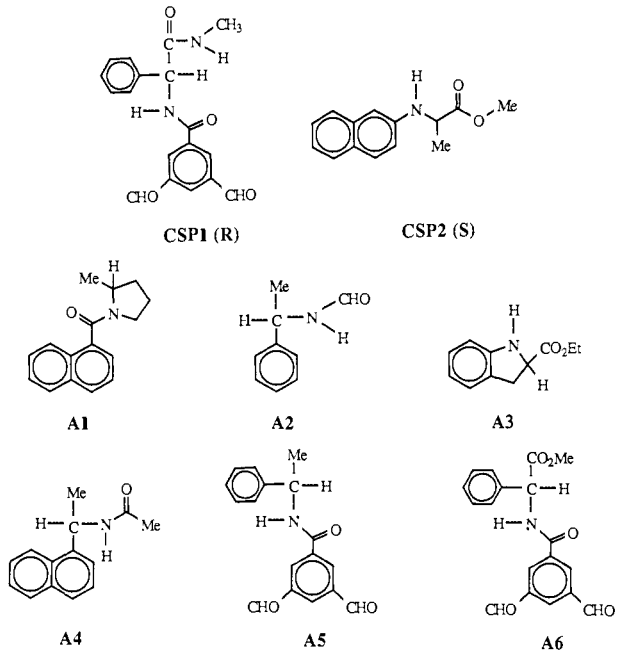

Figure 1.

organic molecules that can adopt multiple conformations, each of which can interact with passing analyte in a unique way. It also accounts for the conformational flexibility of the analyte. Our method, then, accounts for the probablity that the CSP is in a particular conformation, the probability that the analyte is in a particular conformation, and the probability that the two molecules are oriented in a particular way in the complex.

The CSP analogues in Figure 1 have been determined to be very flexible;[14,15] they can adopt several different conformational states at ambient chromatographic conditions as can the analytes that coordinate with them. Furthermore, by virtue of binding by weak dispersion forces or hydrogen bonding, the intermolecular potential energy surfaces for these complexes are relatively flat.[11] To define the averaged dynamic surface area we introduce eq 2 for $\bar{S}_D$, the solvent-accessible surface area, averaged over all available conformations:

$$\bar{S}_D = \sum_{h=1}^{l}\sum_{i=1}^{m}\left(\frac{e^{-E_{CSP,h}/kT}}{\sum_{h'=1}^{l} e^{-E_{CSP,h'}/kT}}\right)\left(\frac{e^{-E_{A,i}/kT}}{\sum_{i'=1}^{m} e^{-E_{A,i'}/kT}}\right)\sum_{j=1}^{n} s_{hij}\left(\frac{e^{-\epsilon_{hij}/kT}}{\sum_{j'=1}^{n} e^{-\epsilon_{hij'}/kT}}\right) \quad (2)$$

As in eq 1, the first factor is the probability of finding the CSP in a given conformation with energy $E_{CSP,h}$, the second factor is the probability of finding the analyte in a particular conformation with energy $E_{A,i}$, and the final factor is the probability of finding the analyte in a particular orientation about the phase. The quantity s_{hij} is the solvent-accessible surface area for each microstate (a microstate is any unique structure of the complex) that is computed with the original Lee and Richards algorithm.[5] The surface area of each microstate is thus weighted by its probability of existing, which, in turn, depends upon its energy, ϵ_{hij}.

Because we anticipate measuring small differences in surface areas we wanted to ensure that the approximate numerical estimates, represented by the Lee and Richards algorithm, reduce adequately the computational error to make these differences significant. Consequently, we employed a smaller than standard sectioning to reduce this error. The standard grid size is 0.25 Å. We employed a more stringent criterion of 0.10 Å.

(14) Lipkowitz, K. B.; Demeter, D. A.; Parish, C. A.; Landwer, J. M.; Darden, T. *J. Comput. Chem.* **1987**, *8*(6), 753–60.
(15) Lipkowitz, K. B.; Demeter, D. A.; Landwer, J. M.; Parish, C. A.; Darden, T. *J. Comput. Chem.* **1988**, *9*(1), 63–66.

Table I. Solvent-Accessible Surface Areas

complex desig[a]	$\bar{S}_D$, Å^2	S_S, Å^2	mean ± SD, Å^2	var in dynamic surf areas, Å^2: lowest s_{hij}	highest s_{hij}
CSP1·A1(*RR*)	642.6	650.2	631.9 ± 11.4	619.6	653.7
CSP1·A1(*RS*)*	643.7	648.1	635.9 ± 10.6	620.3	653.2
CSP1·A2(*RR*)	551.9	552.7	547.7 ± 5.1	536.9	556.6
CSP1·A2(*RS*)*	551.9	552.6	548.2 ± 5.2	536.5	558.0
CSP1·A3(*RR*)	596.2	588.9	592.7 ± 9.3	575.7	607.4
CSP1·A3(*RS*)*	597.8	604.0	593.5 ± 9.4	577.4	607.5
CSP1·A4(*RR*)	615.5	618.2	608.7 ± 6.6	595.2	620.2
CSP1·A4(*RS*)*	615.5	617.9	609.3 ± 7.1	593.0	621.7
CSP2·A5(*SR*)	584.9	579.9	585.9 ± 7.1	570.7	601.2
CSP2·A5(*SS*)*	585.4	584.5	586.5 ± 6.6	570.6	601.9
CSP2·A6(*SR*)	630.9	636.2	632.9 ± 8.2	618.0	646.4
CSP2·A6(*SS*)*	633.1	633.8	633.9 ± 9.6	617.2	646.1

[a] The more stable complex is designated by an asterisk.

The microstates used to determine $\bar{E}$ and $\bar{S}_D$ are obtained by sampling configurations as the analyte is rolled over the van der Waals surface of the CSP.[16] Typically 10^5–10^6 configurations are sampled for the *RR* complex and an equal number for the corresponding *RS* complex. The energy of each microstate is computed with a suitable empirical force field. The MM2 force field with bond moments changed to atom-centered charges was used as explained earlier.[11] The free energy differences, $\Delta\bar{E}$, between *R* and *S* analyte binding to Pirkle phases has been computed with eq 1.[11] The agreement between experiment and theory is good.[12]

Not all microstates used for computing $\bar{E}$ were used in the analysis of $\bar{S}_D$; there simply are too many to consider. Consequently, we used only those microstates within 2 kcal mol^{-1} of the global minimum on the potential energy surface for each diastereomeric complex. A 2 kcal mol^{-1} cutoff retained the microstates that give 90% of the contribution to the energy $\bar{E}$. It is assumed that the other microstates contributing the remaining 10% to $\bar{E}$ will not change the results of $\bar{S}_D$ very much. The most stable structure, i.e., the one with the highest probability of existing, is the global minimum on the complex's potential energy surface. The global minimum for both the *RR* and the *RS* diastereomers of the complexes considered was used as input to the Lee and Richards algorithm to compute the static solvent-accessible surface area, S_S.

Results and Discussion

The results of the calculations for the static and averaged dynamic surface areas are presented in Table I. The first column in the table designates the complex. For example, consider the first entry, CSP1·A1(*RR*). This means analyte A1 is bound to CSP1. The letters in parentheses indicate which diastereomeric complex is considered (the first letter corresponds to the configuration of the phase and the second corresponds to the configuration of the analyte). The second column lists the averaged solvent-accessible surface areas, $\bar{S}_D$, as determined by eq 2. The third column lists the static solvent-accessible surface areas, S_S. These values are the surface areas of the most stable structure for each complex, i.e., of the global minimum. The fourth column lists the mean and standard deviation for the normal curve distribution of states, and the last column indicates the value of the smallest and the largest surface areas of all the microstates used to determine $\bar{S}_D$. These latter values are raw surface areas, i.e., the s_{hij} that have not been scaled by their probabilities; they are given only to show the range of values that can be achieved by conformational fluctuations. The more stable of the two dia-

(16) A variety of methods exist for sampling configurations. At first we intended to use molecular dynamics but found that unrealistically high tempertures were needed to ensure sampling of all analyte orientations around the CSP. Consequently, we use a deterministic sampling approach that ensures all major configurations of both CSP and analyte are considered as well as ensuring all orientations of analyte with respect to CSP have been sampled. For details see ref 10.

Table II. Polar and Nonpolar Contributions to $\bar{S}_D$

complex desig	satd solvent-accessible surf, Å^2	unsaturated solvent-accessible surf, Å^2	polar solvent-accessible surf, Å^2
CSP1·A1(*RR*)	347.1	154.4	141.1
CSP1·A1(*RS*)*	346.5	155.1	142.2
CSP1·A2(*RR*)	265.2	128.6	158.2
CSP1·A2(*RS*)*	265.5	128.5	157.8
CSP1·A3(*RR*)	301.8	129.9	164.5
CSP1·A3(*RS*)*	301.9	131.7	164.3
CSP1·A4(*RR*)	310.7	152.9	151.9
CSP1·A4(*RS*)*	311.1	152.5	151.9
CSP2·A5(*SR*)	310.1	146.5	128.2
CSP2·A5(*SS*)*	310.5	146.4	128.5
CSP2·A6(*SR*)	313.1	156.9	161.0
CSP2·A6(*SS*)*	313.0	159.5	160.5

[a] The more stable complex is designated by an asterisk.

stereomeric complexes for each entry is the one with the asterisk. In Table I the surface areas listed are total solvent-accessible surface areas. The total surface area $\bar{S}_D$ has been partitioned into polar and nonpolar contributions in Table II.

Before discussing these results, one may speculate what to expect. It might be intuitively anticipated that the more stable of the two complexes would have the smaller surface area. This presumes that the more stable complex has the analyte more tightly held to the CSP, resulting in a complex that is physically smaller than the less stable complex. Is this chemical intuition correct?

In all cases the $\bar{S}_D$ of the most stable complex is equal to or greater than $\bar{S}_D$ of the less stable complex. This was not expected and one would be inclined to dismiss these findings as meaningless results due to an artifact in the computational method. However, the results of our simulations portray the following picture which also intuitively makes sense. As two molecules encounter one another to form a complex, on average, the more unfolded the molecules become, the greater will be the dispersion attraction between them. This is most evident in simple hydrocarbons where branching lowers alkane boiling points (the molecules assume more of a spherical shape, reducing the London forces holding the liquid together). The more extended molecules, in turn, give rise to a larger solvent-accessible surface area. We now compare these findings with the results from static surface areas.

A perusal of Table I indicates no consistent trend with regard to the size of the more stable complex. For entries 3 and 5 we see the more stable complex to have the larger static surface areas, in agreement with the $\bar{S}_D$ results, but for the other entries we find the more stable complex to display smaller static surface areas. These inconsistencies are rationalized by considering the variation in dynamic surface areas listed in Table I. Consider, for example, the first entry. The fluctuation among unaveraged solvent-accessible surface areas is 34.1 Å^2 for the *RR* diastereomer and 32.9 Å^2 for the *RS* diastereomer. Our interest is in measuring the inherent difference between surface areas of weakly bound complexes, ΔS_S. For entry 1 we find the difference between static surface areas, ΔS_S, to be 2.1 Å^2. For this example, therefore, the variation among unaveraged surface areas far exceeds the difference between static surface areas of the *RR* vs *RS* diastereomers. Indeed for this and the remaining five entries in Table I the "noise" (variation in s_{hij}) is larger than the "measurement" being made (ΔS_S).

The results of S_S presented in Table I are therefore construed to have little meaning. We find a large number of microstates close in energy to the global minimum and these states correspond to structures with vastly different static solvent-accessible surface areas. Selecting a single structure or conformer of a molecule to be used for calculation of static surface areas thus could be inappropriate and misleading. This is always a risk one encounters when using one of many possible structures to describe the state of a system. It is expected, then, that this problem would not exist for statistically averaged values and that meaningful results are obtained.

The dependence of surface area upon molecular conformation has already been noted by several authors.[17] In a paper describing the effect of internal rotation on surface and volumes of small organic molecules, Bleha plotted surface areas as a function of dihedral angle.[18] Although the internal strain energies of the molecules were not plotted along with the surface areas, it appears that high-energy, congested conformations, as expected, give smaller surface areas and volumes. It was pointed out, however, that a direct correlation between surface area and conformational energy does not always hold and that using computed van der Waals surfaces to predict stable conformations of molecules is limited.

The fluctuations in surface area of the conformations studied by Bleha were relatively small (in the 3% range) and deemed rather inconspicuous. The difference between stable rotamers was even smaller. For the weakly bound complexes in our study we find a larger variation. For all complexes listed in Table I the variation in surface area is between 4% and 6% of $\bar{S}_D$. Our motive for determining solvent-accessible surface areas is to begin addressing the issue of differential solvation. It has been amply demonstrated that solvent-accessible surface areas correlate with experimental partition coefficients.[19] It is clear, however, that using static surfaces is risky, especially for determining solvation enthalpies with continuum models.[20] It would be more appropriate to use averaged structures.

It has been suggested for amino acid side chains that each Å^2 removed from contact with water to a more hydrocarbon-like environment results in a free energy gain of 20–30 cal.[21] Transfer into an ethanol or dioxane medium gives 20–24 cal for each Å^2 removed from water while these values are ~20% higher for hydrocarbon media. This assessment was made by correlating the free energy of transfer of amino acids determined experimentally with computed solvent-accessible surface areas.[21] The computed values were static surface areas and, because of the large fluctuations in static surface areas noted above, it is not clear how meaningful these numbers are. Nevertheless by using these values and observing the $\bar{S}_D$ in Table I, where the difference, $\Delta\bar{S}_D$, for competing diastereomeric complexes is between 0.0 and 2.3 Å^2, we can expect differential solvation free energies far less than kT. These small differences in solvation energies may at first seem inconsequential, but it is to be noted that the inherent difference in free energies for analyte binding to CSP's 1 and 2 is usually only an order of magnitude larger. Differential solvation of the transient diastereomeric complexes that form during chiral chromatography should, therefore, be very important. We should also point out that the analyte and the CSP in uncomplexed form are also interacting with the mobile phase. With the Pirkle-type CSPs and a hexane/alcohol mobile phase, one can assume that the analyte approaches a CSP coated with the polar modifier. The relative retention of the analyte on the CSP is, in part, a function of the ability of the analyte to displace the modifier from the surface of the CSP. This affects stereochemical resolution which has been pointed out for the Pirkle-like CSPs by a number of groups[22] and for other types of CSPs.[23] In all of the modeling to date we have omitted this fact by assuming the *R* and *S* analytes have nearly similar abilities to displace the modifier. This may

(17) (a) Christian, S. D.; Grundes, J.; Klaboe, P. *J. Chem. Phys.* **1976**, *65*, 496. (b) Schoen, P. E.; Priest, R. G.; Sheriden, J. P.; Schnur, J. M. *J. Chem. Phys.* **1979**, *71*, 317. (c) Taniguchi, Y.; Takaya, H.; Wong, P. T. T.; Whalley, E. *J. Chem. Phys.* **1981**, *75*, 4815. (d) Pratt, L. R.; Hsu, C. S.; Chandler, D. *J. Chem. Phys.* **1978**, *68*, 4202. (e) Bleha, T.; Gajdos, J.; Tvaroska, I. *J. Mol. Struct.* **1980**, *68*, 189.

(18) Bleha, T. *Chem. Zvesti* **1984**, *38*(2), 181–88.

(19) (a) Camilleri, P.; Watts, S. A.; Borasten, J. A. *J. Chem. Soc., Perkin Trans. 2* **1988**, 1699–1707. (b) Funasaki, N.; Hada, S.; Neya, S. *J. Phys. Chem.* **1985**, *89*, 3046–49 and references therein.

(20) See, for example, the method proposed by Rashin: Rashin, A. A.; Namboodiri, K. *J. Phys. Chem.* **1987**, *91*, 6003 and references cited.

(21) Chothia, C. *Nature* **1975**, *254*, 304–8.

(22) (a) Zief, M.; Crane, L. J.; Horvath, J. *J. Liq. Chromatogr.* **1984**, *7*(4), 709–30. (b) Pescher, M. C.; Rosset, R.; Tambute, A. *J. Chromatogr.* **1986**, *371*, 159–175. (c) Macaudiere, P.; Tambute, A.; Caude, M.; Rosset, R.; Alembik, M. A.; Wainer, I. W. *Ibid* **1968**, *371*, 177–193.

(23) See especially the chapter by Zief in ref 9b.

be incorrect and merits investigation.

The total dynamic solvent-accessible surface areas for the complexes studied have been partitioned into three components in Table II. The numbers listed in Table II are statistically averaged values that, upon summation, provide the $\bar{S}_D$ numbers listed in Table I. The first column in Table II is the solvent-accessible surface area attributed to the saturated (alkane) hydrocarbon portion of the complex, the second column is the solvent-accessible surface area attributed to the unsaturated (aromatic) portion, and the last column is that solvent-accessible surface area attributed to the polar (heteroatoms) portion of the complex's van der Waals surface. The sum of the saturated and unsaturated components is thus the lipophilic contribution to the total solvent-accessible surface area. These terms were computed in an attempt to see if any trends are apparent. We wondered, for example, if the more stable diastereomer, on average, had more or less polar surface area than the less stable diastereomer.

In Table II we see the saturated solvent-accessible surface areas contribute between 48% and 54% of the total dynamic area. The unsaturated solvent-accessible surface areas contribute 22–25% to the total while the polar contribution is between 22% and 29%. As a generalization, then, one can say that the solvent-accessible surfaces of these complexes are mainly hydrocarbon-like and that nearly one-quarter of the surface has a polar make-up. These results are about what one would expect upon inspection of the molecules in Figure 1.

Differences between the competing diastereomeric complexes listed in entries 1–6 in Table II exist but there are no general trends. For entries 1 and 2 we observe the largest difference between diastereomers to be mainly polar. On the other hand, for entries 3 and 6 the largest differences between diastereomers involve the unsaturated surface areas, and for entries 4 and 5 the largest difference between competing diastereomers shows up in the saturated surface areas. While no trends exist, one may anticipate that the complexes that differ most in their polar solvent-accessible surface areas should be most influenced by polar solvents. Thus we expect to see CSP1·A1 and CSP1·A2 most influenced by polar solvents. Our prediction, then, is that the separation of A1 and A2 on CSP1 will be most sensitive to changes in polar cosolvent. We are exploring this experimentally.

Conclusions

The results of our simulations convey the following picture. As two molecules in their bundled-up, minimum-energy conformations encounter one another they tend to unravel somewhat to maximize the attractive dispersion forces with their partners. Unraveling from a low-energy conformation to a less stable form is offset by the gain in energy from complexation. For the weak complexes studied here the more stable of the two diastereomeric complexes have the CSP and the analyte most unraveled and furthest extended. This enhances substrate binding and it results in the more stable diastereomeric complex having the larger solvent-accessible surface areas.

The purpose of this study was to assess the inherent differences between surface areas of weakly bound diastereomeric complexes. By using the traditional approach of locating the most stable structure for each complex and computing the corresponding solvent-accessible surface area, S_S, we find differences between the diastereomeric surfaces, ΔS_S, to be smaller than the variation in fluctuations the complexes can achieve at any given instant. That is to say, with the traditional approach the noise is larger than the measurements being made and inconsistent results are obtained. Averaging these fluctuations in an energy-weighted way circumvents this problem and gives more meaningful results. These averaged dynamic surface areas, $\bar{S}_D$, were used to estimate differential solvation free energies. It is found for weakly bound diastereomeric complexes that the differential solvation energies are within an order of magnitude of the differential free energies of analyte binding and that solvent conditions could play a major role in analyte resolution.

Acknowledgment. Helpful discussions with Don Boyd at Eli Lilly and Co. are greatly appreciated. This work was funded by the donors of the Petroleum Research Fund, administered by the American Chemical Society, and by a grant from the National Science Foundation (CHE-8901828).